For the over-all $^{11}B/^{10}B$ ratio, one must consider the production of ^{11}B and ^{10}B separately from all the targets, weighted by the appropriate abundances. The solar photospheric abundances of the important targets ^{12}C, ^{14}N, and ^{16}O are in the approximate ratios 3:1:5.[16] Because of differing values of production thresholds, each of these three targets might be expected to contribute about equally to the formation of ^{11}B and ^{10}B. Preliminary values obtained in this laboratory for the $^{11}B/^{10}B$ ratios at 35 MeV for ^{14}N and ^{16}O are 0.5 and 8, respectively. Below 12 MeV only ^{11}B is produced from ^{14}N, via the $^{14}N(p,\alpha)^{11}C$ reaction. These results are consistent with the suggestion of Bernas *et al.*[11] that the solar system $^{11}B/^{10}B$ formation ratio has not been altered by subsequent nuclear processes.

The low value of the ^{9}Be production cross section is not surprising, in view of the fact that this nucleus has only one particle-stable state, compared to the nine or so states available in ^{11}B and ^{11}C. In addition, the formation of ^{9}Be via the direct $(p, p^{3}He)$ reaction is expected to depend strongly on the probability of finding ^{3}He clusters in the target nucleus, a situation likely to occur only infrequently.

Production of ^{7}Li from ^{12}C exceeds that of ^{6}Li by a factor of 2–3, in agreement with the estimates of Barnas *et al.*[11] A large $^{7}Li/^{6}Li$ ratio near threshold was not observed. Such a large ratio might have made it possible to explain the terrestrial and meteoritic $^{7}Li/^{6}Li$ ratio if, in addition, a spectrum of protons with energies extending only to about 25 MeV were postulated. The necessity of a secondary process to explain the terrestrial $^{7}Li/^{6}Li$ ratio remains, the most likely candidate being the $^{6}Li(p,\alpha)$ reaction. Slow neutrons do not seem to be the answer, since they would increase the $^{11}B/^{10}B$ ratio further.

Further measurements of proton spallation cross sections for LiBeB production from ^{14}N, ^{16}O, and heavier targets, as well as additional measurements on ^{12}C at higher energies, are required. It is hoped that such results will soon be available, enabling a better understanding of the origin of lithium, beryllium, and boron.

[16] E. A. Muller, in *Origin and Distribution of the Elements*, edited by L. H. Ahrens (Pergamon Press, Oxford, 1968), p. 155.

PHYSICAL REVIEW C VOLUME 1, NUMBER 1 JANUARY 1970

(d, p) and (d, t) Reaction Studies of the Actinide Elements. I. U^{235} †

T. H. Braid, R. R. Chasman, J. R. Erskine, and A. M. Friedman
Argonne National Laboratory, Argonne, Illinois 60439

(Received 2 September 1969)

Levels of the nucleus U^{235}, populated in the reactions $U^{234}(d, p)U^{235}$ and $U^{236}(d, t)U^{235}$ induced by 12-MeV deuterons from the Argonne tandem Van de Graaff, were analyzed with a magnetic spectrograph. Most of the observed levels were identified as members of rotational bands built on the single-particle states of a deformed central field. The level assignments were made on the basis of relative populations of presumed members of each rotational band, ratios of the cross sections at 90° and 140°, and $(d, p)/(d, t)$ cross-section ratios. Pairing effects were calculated for the observed spectrum, and a single-particle scheme was extracted from the data. This single-particle scheme was compared with the calculations of Nilsson and Rost. Levels not predicted on the basis of the single-particle models were observed at excitations as low as 700 keV. Some of these levels, presumably vibrational excitations, were found to have cross sections comparable to those of single-particle states.

I. INTRODUCTION

In this paper, we report the results of an investigation of (d, p) and (d, t) reactions populating levels in U^{235}. The considerations that govern these single-neutron transfer reactions are quite different from those applicable to decay processes, and accordingly these studies have furnished a large amount of new information on levels in U^{235}. The differential cross sections measured for these reactions give detailed information which is not readily obtained in other ways. Our measurements, in conjunction with results obtained from α-decay[1–3] and Coulomb-excitation[4,5] studies of U^{235}, give a rather extensive picture of the low-energy excitations in this nucleus. We shall examine this picture in the present paper. In future papers, we shall utilize our (d, p) and (d, t) data to analyze levels in the

† Work performed under the auspices of the U.S. Atomic Energy Commission.

[1] S. A. Baranov, V. M. Koulakov, and S. N. Belenki, Nucl. Phys. **41**, 95 (1963).
[2] Irshad Ahmad, Ph.D.thesis, University of California Lawrence Radiation Laboratory Report No. UCRL-16888, 1966 (unpublished).
[3] J. E. Cline, Nucl. Phys. **A106**, 481 (1968).
[4] J. O. Newton, Nucl. Phys. **3**, 345 (1957).
[5] F. S. Stephens, M. D. Holtz, R. M. Diamond, and J. O. Newton, University of California Lawrence Radiation Laboratory Report No. UCRL-17976, 1968 (unpublished); Nucl. Phys. **A115**, 129 (1968).

nuclides Th^{229}, Th^{231}, Th^{233}, U^{233}, U^{237}, U^{239}, Pu^{241}, Pu^{243}, Cm^{243}, Cm^{245}, Cm^{247}, and Cm^{249}. Preliminary reports of the results of our reaction studies have been presented.[6–10]

The experimental facilities involved in the measurement of (d, p) and (d, t) reaction cross sections have included a tandem Van de Graaff as a source of monoenergetic deuterons, a broad-range magnetic spectrograph for high-precision measurement of the energies of emitted protons and tritons, and an isotope separator for the preparation of thin uniform targets.

Section II is a discussion of the theoretical framework within which our reaction studies are analyzed. In Sec. III, we discuss experimental procedures and techniques. In Sec. IV, we present our experimental results. The levels in U^{235} are analyzed in Sec. V, and the single-particle level scheme extracted from this analysis is given. Section VI is a summary, and the Appendix consists of a discussion of actinide deformations obtained from Coulomb-excitation measurements.

II. THEORETICAL ANALYSIS

A major purpose of the experiments reported here is to establish a neutron single-particle level scheme. The theoretical framework for the analysis is not exhaustive; consequently, quantitative agreement between calculated and experimental results is neither expected nor obtained. The present paper reports an experimental examination of the levels of U^{235} populated by the reactions $U^{234}(d, p)U^{235}$ and $U^{236}(d, t)U^{235}$.

We assume that the differential cross section can be factored into two parts, one depending on the reaction mechanism and the other on the nature of the nuclear eigenstates. This approximation can be written

$$d\sigma/d\Omega = (2J+1)\, S_J{}^{\kappa} \Theta_J{}^{\mathrm{DW}} \qquad (1)$$

for a (d, p) or (d, t) reaction on an even-even target, where J denotes the total angular momentum of the final state, the index κ denotes the specific state being populated, the quantity $\Theta_J{}^{\mathrm{DW}}$ is the single-nucleon-transfer cross section which we have calculated by using the distorted-wave Born approximation (DWBA),[11] and $S_J{}^{\kappa}$ is the spectroscopic factor which depends only on the details of the eigenstates of the target and recoiling nucleus. The single-nucleon-transfer cross sections were calculated with the DWBA code JULIE.[12] A discussion of our use of this code follows at the end of this section.

The spectroscopic factor $S_J{}^{\kappa}$ is calculated with the aid of the collective model which has been so successful in explaining the properties of the actinide elements. The nuclear Hamiltonian used is of the form

$$H = H_{\mathrm{s.p.}} + H_{\mathrm{pairing}} + H_{\mathrm{rotor}},$$

where $H_{\mathrm{s.p.}}$ denotes a single-particle Hamiltonian whose potential is axially symmetric. We have, in fact, considered two different calculations of single-particle energies—those of Nilsson[13] and Rost.[14] The single-particle wave functions obtained from these models yield predictions of the relative probabilities with which transfer reactions populate the members of the rotational band based on each single-particle state. We refer to this pattern of relative populations as the signature of the single-particle state. The Nilsson wave functions are of the form

$$\chi_a{}^{\Omega} = \textstyle\sum_J C_{J,l}{}^{a} \psi_{J,l}, \qquad (2)$$

where the basis functions $\psi_{J,l}$ are spherical oscillator eigenstates.

In the Rost calculation, the single-particle potential is a deformed Woods-Saxon well. We have made use of two different Rost computer programs.[15] The first uses a method similar to the Nilsson calculation and gives expansion coefficients which are analogous to the Nilsson $C_{jl}{}^{a}$ of Eq. (2). The basis functions are states of the spherical Woods-Saxon potential. The second method uses a coupled-channel procedure[14] and gives wave functions of the form

$$\chi_a{}^{\Omega} = r^{-1} \sum_{J,l,\Omega} u_{J,l,\Omega}(r)\, |J, l, \Omega\rangle, \qquad (3)$$

where the radial functions $u_{J,l,\Omega}(r)$ are determined by a coupled-channel calculation for each deformation and $|J, l, \Omega\rangle$ is a spin-angle eigenfunction. For the analysis of our reaction studies, the quantities

$$(C_{J,l}{}^{a})^2 \quad \text{and/or} \quad \int_0^{\infty} [u_{J,l,\Omega}(r)]^2 dr$$

are essential. The relative differential cross sections of the members of the rotational bands are proportional to these quantities (except for DWBA factors). The signature predictions of Nilsson and either Rost calculation are quite similar, and our experimental results do not indicate that one calculation is generally superior to the other.

The effect of the pairing term in our Hamiltonian becomes apparent when we consider the theoretical expression for the ratio R_{κ} of (d, p) to (d, t) spectro-

[6] T. H. Braid, R. R. Chasman, J. R. Erskine, and A. M. Friedman, Phys. Letters **18**, 149 (1965).
[7] A. M. Friedman, J. R. Erskine, and T. H. Braid, Bull. Am. Phys. Soc. **10**, 540 (1965).
[8] J. R. Erskine, A. M. Friedman, and T. H. Braid, Bull. Am. Phys. Soc. **10**, 40 (1965).
[9] J. R. Erskine, A. M. Friedman, T. H. Braid, and R. R. Chasman, in *Proceedings of the Third International Conference on Atomic Masses* (University of Manitoba Press, Winnipeg, 1967).
[10] J. R. Erskine, A. M. Friedman, T. H. Braid, and R. R. Chasman, in International Symposium on Nuclear Structure, Dubna, 1968 (unpublished), contributed paper No. 61.
[11] G. R. Satchler, Nucl Phys. **55**, 1 (1964).
[12] R. H. Bassel, R. M. Drisko, and G. R. Satchler, Oak Ridge National Laboratory Report No. ORNL-3240 (unpublished).
[13] S. G. Nilsson, Kgl. Danske Videnskab. Selskab, Mat.-Fys. Medd. **29**, No. 16 (1955).
[14] E. Rost, Phys. Rev. **154**, 994 (1967).
[15] We are indebted to E. Rost for graciously making his computer codes available for our use.

TABLE I. Optical-model parameters used in the DWBA calculations.

Particle	V_0 (MeV)	W (MeV)	r_0 (F)	r_c (F)	a (F)	λ	r_0' (F)	a' (F)	W' (MeV)
d	60	15	1.5	1.5	0.6				
p	57	8	1.3	1.3	0.5				
t	155	0	1.2	1.2	0.7		1.30	0.65	40
n			1.25	1.25	0.65	25			

scopic factors. This ratio, which arises from pairing considerations, is given by

$$R_\kappa = \frac{S_J{}^\kappa(d,p)}{S_J{}^\kappa(d,t)} = \frac{\langle\phi_\kappa(A)\mid a_\kappa{}^+\mid\phi_0(A-1)\rangle^2}{\langle\phi_\kappa(A)\mid a_{-\kappa}\mid\phi_0(A+1)\rangle^2}\approx\frac{1-\langle N_\kappa(A-1)\rangle}{\langle N_\kappa(A+1)\rangle}, \quad (4)$$

where ϕ_κ indicates the state in which the single-particle level κ is blocked, $\phi_0(A\pm1)$ designates the ground state of the even-even target having $A\pm1$ nucleons, and $\langle N_\kappa(A\pm1)\rangle$ indicates an occupation probability in the appropriate ground state. Qualitatively, Eq. (4) tells us that $R_\kappa>1$ for particle states and $R_\kappa<1$ for hole states. R_κ goes to infinity for particle states at high excitation and approaches zero for hole states far below the Fermi surface. In this way, consideration of the (d,p) and (d,t) cross-section data immediately removes one ambiguity in the analysis of single-particle levels.

From the single-particle and pairing terms in our Hamiltonian, we obtain spectroscopic factors

$$S_J{}^\kappa\approx[2/(2J+1)](C_{J,l}{}^\kappa)^2[1-\langle N_\kappa(A-1)\rangle] \quad (5)$$

for (d,p) reactions and

$$S_J{}^\kappa\approx[2/(2J+1)](C_{J,l}{}^\kappa)^2\langle N_\kappa(A+1)\rangle \quad (6)$$

in the case of (d,t) reactions. In place of the Nilsson $(C_{J,l}{}^\kappa)^2$, we can also use the Rost integral

$$\int_0^\infty[u_{J,l,\Omega}(r)]^2dr.$$

Equations (5) and (6) can be substituted into Eq. (1) to obtain the familiar expressions for the differential cross section,[16] namely,

$$d\sigma^\kappa(d,p)/d\Omega=2(C_{J,l}{}^\kappa)^2[1-\langle N_\kappa(A-1)\rangle]\Theta_J{}^{\mathrm{DW}}(d,p) \quad (7)$$

and

$$d\sigma^\kappa(d,t)/d\Omega=2(C_{J,l}{}^\kappa)^2\langle N_\kappa(A+1)\rangle\Theta_J{}^{\mathrm{DW}}(d,t). \quad (8)$$

The effect of H_{rotor} is to complicate the above picture somewhat. The nonzero matrix elements[17] of H_{rotor} are of the form

$$\langle\alpha,I,\Omega+1\mid H_{\mathrm{rotor}}\mid\beta,I,\Omega\rangle=(\hbar^2/2\mathcal{I})[(I+\Omega)\times(I-\Omega+1)]^{1/2}\sum_J C_J{}^{\Omega+1}(\alpha)C_J{}^\Omega(\beta)[(J+\Omega)\times(J-\Omega+1)]^{1/2}\langle\alpha\mid a_{-\beta}{}^+a_{-\alpha}{}^+a_\alpha{}^+a_\beta\mid\beta\rangle, \quad (9)$$

where the symbols α and β denote two different single-particle states, and the final factor represents a pairing effect which corresponds to $(U_\alpha{}^\beta U_\beta{}^\alpha+V_\alpha{}^\beta V_\beta{}^\alpha)$ in the BCS approximation. The form of Eq. (9) implies that we have first treated pairing effects and then the effects of H_{rotor}; there is some ambiguity in this ordering. The mixing of single-particle states through this interaction can modify the single-particle signatures substantially.

Several parameters enter this analysis of the data. The single-particle wave functions which play a key role in this analysis depend on the parameters of the single-particle potential. We have chosen the potential-well parameters to get good agreement with the experimentally observed level ordering in U^{235}. For the Nilsson-model calculation of single-particle wave functions, we used the conventional[13] values $\kappa=0.05$ and $\mu=0.45$ and chose a deformation $\beta_2=0.25$. For the Rost-model calculation of single-particle wave functions, the relevant parameters are $\beta_2=0.25$, $a=0.67$ F, $R_0=1.33$ F, $\lambda=37.5$, and $V_0=44.2$ MeV. The value of β_2 used in the two calculations is consistent with our Coulomb-excitation measurements described in the Appendix. These measurements are consistent with the results of Skurnik *et al.*[18]

The pairing interaction introduces an additional parameter into the analysis, the pairing interaction constant G. We have used values of G (in MeV) of $21.5/A$–$22.5/A$ in our calculations, and find that R_κ is insensitive to this variation. Thirty levels were used for the pairing calculations. It is also necessary to specify the energies of single-particle states in order to do the pairing calculation. Instead of using the values obtained from single-particle calculations, we have used the experimental data to determine the energies of the single-particle states near the Fermi surface of U^{235}. This was done by varying the input energies until the pairing calculation gave a set of levels that was in agreement with our assignment of states in U^{235}. The set of input energies determined in this way is referred

[16] G. R. Satchler, Ann. Phys. (N.Y.) **3**, 275 (1958).
[17] A. K. Kerman, in *Nuclear Reactions*, edited by P. M. Endt and M. Demeur (North-Holland Publishing Co., Amsterdam, 1959), Vol. I, Chap. X.
[18] E. Z. Skurnik, B. Elbek, and M. C. Olesen, Nucl. Phys. **22**, 316 (1961).

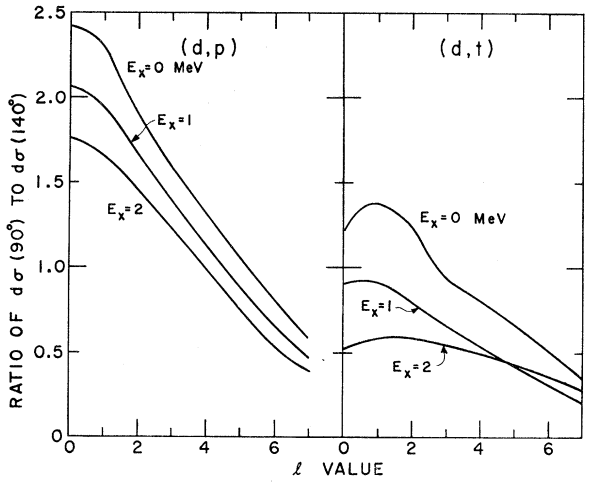

FIG. 1. Calculated values of the ratio of the differential cross section at 90° to that at 140° as a function of angular-momentum transfer l. The values shown are for the $U^{234}(d, p)U^{235}$ and $U^{236}(d, t)U^{235}$ reactions leading to levels of low excitation energy. The bombarding energy was 12 MeV.

to as the extracted single-particle level scheme. In these pairing calculations we used methods described previously.[19]

In utilizing the DWBA code JULIE to calculate $\Theta_{Jl}{}^{DW}$, we used the optical-model parameters shown in Table I. The parameters for protons and deuterons are those of Macefield and Middleton,[20] while those for tritons were from extrapolations given to us by Flynn.[21] No spin-orbit terms were included for the incoming and outgoing particles, but such a term was included in the bound state. Normalization constants 1.65 and 3.33 were used for the (d, p) and (d, t) reactions, respectively.[22]

The basis states for which $\Theta_{Jl}{}^{DW}$ has been calculated are the $3p_{1/2}$, $3p_{3/2}$, $2f_{5/2}$, $2f_{7/2}$, $1h_{9/2}$, $1h_{11/2}$, $2h_{11/2}$, $1j_{13/2}$, and $1j_{15/2}$ odd-parity states and the $4s_{1/2}$, $3d_{3/2}$, $3d_{5/2}$, $2g_{9/2}$, $1i_{11/2}$, and $1i_{13/2}$ even-parity states. Since the targets are even-even, only one value of l, J contributes to the cross section for each level; and for the great majority of the states it is clear that only one principal quantum number should be included. However, for a few levels of odd parity and $J=\frac{9}{2}$ and $\frac{11}{2}$, we have found that the expansion of the wave function in terms of the spherical states of the distorted Woods-Saxon potential allows comparable contributions from two major shells; but only in the case of the $h_{9/2}$ and $h_{11/2}$ states does this have any effect on levels that are strongly excited in the experiment. (The basis levels belonging to $n=1$ and 2 are in this case about equally far removed from the Fermi level, one far above and the other far below.)

[19] R. R. Chasman, Phys. Rev. **134**, B279 (1964).
[20] B. E. F. Macefield and R. Middleton, Nucl. Phys. **59**, 561 (1964).
[21] E. R. Flynn (private communication).
[22] R. H. Bassel, Phys. Rev. **149**, 791 (1966).

The appropriate combination of the Θ_{Jl}'s, which must be used in such cases to calculate the Woods-Saxon signatures, is obtained by using the wave function [Eq. (3)] generated in a coupled-channel calculation[14] as the form factor in JULIE instead of the spherical wave functions. Since in this region significant mixing of basis states was found only for the odd-parity states mentioned above, the calculations were made in this fashion for all the levels in the odd-parity bands ($N=5$ and 7) while the even-parity bands (and bands of both parities in the Nilsson case) were calculated in the conventional manner.

In general, we believe that while there are considerable uncertainties in the calculation of Θ_{Jl} from the DWBA in this region of the Periodic Table (especially in the *absolute* values), the numbers obtained are good enough for the qualitative use we make of them in this paper.

Figure 1 is a plot of the calculated values of $d\sigma(90°)/d\sigma(140°)$ as a function of the transferred angular momentum. It was pointed out by Macefield and Middleton[20] that this ratio decreases with increasing l. We have found that this ratio is much less sensitive to the parameters than are the values of the cross sections themselves. For levels populated with sufficiently large cross sections, we have used this ratio as a guide in attempting to infer spins.

III. EXPERIMENTAL PROCEDURE

A 12-MeV deuteron beam, obtained from the Argonne tandem Van de Graaff, was used in these experiments. The reaction products were analyzed with a Browne-Buechner-type broad-range magnetic spectrograph which has been described elsewhere.[23] The solid angle accepted by the spectrograph was increased to about 10^{-3} sr by removing the zone-defining masks that normally are placed in front of the nuclear emulsion. A strip of emulsion approximately 3 cm wide could then be exposed. During the (d, p) exposures, foils of cellulose triacetate were placed over the emulsions to stop elastically scattered deuterons.

Because of the intense natural α activity of some of the targets, it was found necessary to design a special target holder in order to minimize the danger of accidental contamination of personnel and equipment. The targets were supported on 20–40-$\mu g/cm^2$ films of carbon which were backed with 10–20-$\mu g/cm^2$ films of Formvar. It has been found that if a carbon-Formvar film of this type breaks, it will curl up onto the frame rather than scatter around the chamber. The films were suspended over a 3×12-mm aperture in a platinum sheet which was cemented to a standard target frame. The size of the beam spot was $\sim0.5\times5$ mm. The targets were mounted in a removable shell that served both as a liner for the scattering chamber during

[23] J. R. Erskine, Phys. Rev. **135**, B110 (1964).

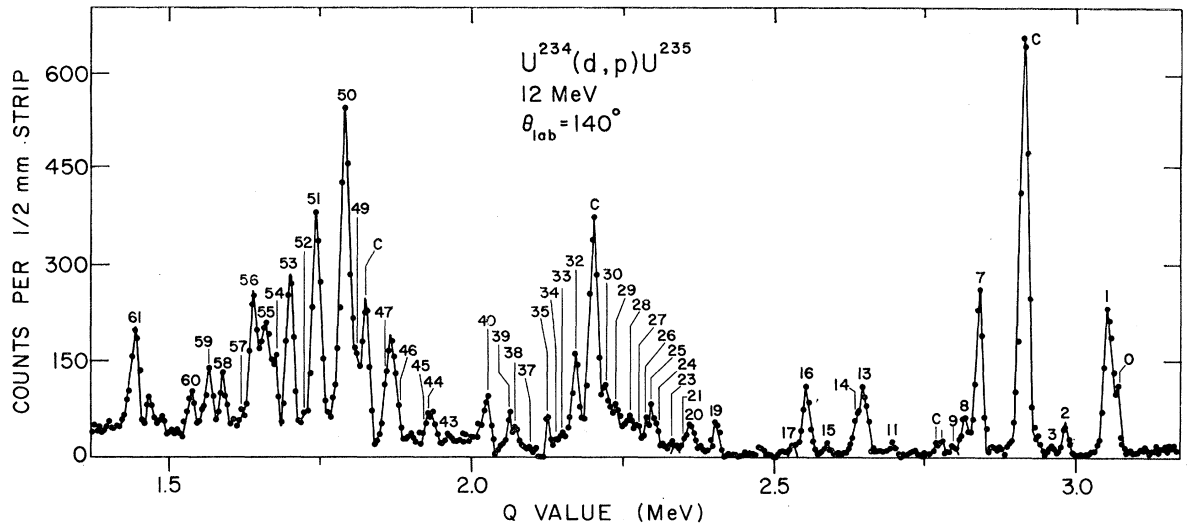

FIG. 2. Spectrum of protons observed at 140° from a U^{234} target bombarded with a 12-MeV deuteron beam. Contaminant peaks are labeled C. Other spectra were obtained with no contaminant peaks but with smaller yields.

experiments and as a container for transporting the targets between the "hot lab" and the tandem target room. The only openings into this liner are a set of slots through which the beam enters and leaves the liner and through which the reaction products reach the spectrograph and monitor. The target can be accurately and reproducibly positioned in the beam with the aid of an external micrometer. Before each experiment the target was adjusted with the micrometer to maximize the amount of beam scattered into a silicon-surface-barrier detector mounted at 90° to the beam while minimizing the scattering from the edges of the target frame. In one experiment, a Cm^{244} target having 10^{10} α disintegrations/min was used. No detectable α contamination was found in the scattering chamber after the bombardment.

The targets were prepared by two methods. Our most successful targets were those prepared by Lerner[24] with the Argonne Experimental Isotope Separator, which is similar to the one described by Alväger and Uhler.[25] The isotopes in the beam from the separator were deposited directly onto the backings. A multiple-beam retarder was used to increase the rate of accumulation of collected material and to prepare several targets of different isotopes simultaneously. Targets with thicknesses from 20 to 500 $\mu g/cm^2$ were made in this way. Since the target material was deposited in a spot approximately 0.8×6 mm (similar in size to the beam spot from the tandem), a sufficiently thick target could be made with a minimum of target material—a decided advantage when working with radioactive targets. Previously, targets had been made with a modification of the electrospraying technique developed by Carswell and Milsted.[26] In this technique, a solution of uranyl acetate dissolved in acetone is placed in a fine glass capillary along with a platinum wire electrode. The electrode is connected to a positive 1200-V power supply and the target frame is connected to the ground of the supply. When the glass capillary is brought within 1 cm of the carbon film, a spray of very fine droplets of the solution is pulled from the capillary by the field and impinges upon the carbon film. During the spraying process, the film is oscillated about the tip and heated with an infrared lamp to ensure uniformity of the deposit. After a 30–50-$\mu g/cm^2$ layer of uranyl acetate is built upon the film, the film and frame are placed in an oven and heated gently to 300°C to convert the acetate to uranium oxide. By repeating the process, targets of any desired thickness up to a few mg/cm^2 can be prepared. For the uranium targets we tried to obtain 70–80 $\mu g/cm^2$ of uranium since increased thickness decreased our over-all resolution. The separated isotopes were furnished by the Isotope Division of Oak Ridge National Laboratory and further enriched with the Argonne Experimental Isotope Separator.

The output of the monitor detector at 90° to the beam was observed with a multichannel analyzer and was also connected to a single-channel analyzer and scaler. The multichannel analyzer was used in adjusting the target position to minimize scattering from the target frame. The window of the single-channel analyzer was set to measure only the elastically scattered deuteron peak from the uranium target, and the scaler counted these throughout each experiment. The absolute differential cross section was determined from the known solid angles of the monitor and spectrograph and the calculated differential cross section for elastic scattering.

[24] We are indebted to J. Lerner for the preparation of these targets.

[25] T. Alväger and J. Uhler, Arkiv Fysik **13**, 145 (1958).

[26] D. J. Carswell and J. Milsted, J. Nucl. Energy I **4**, 51 (1957).

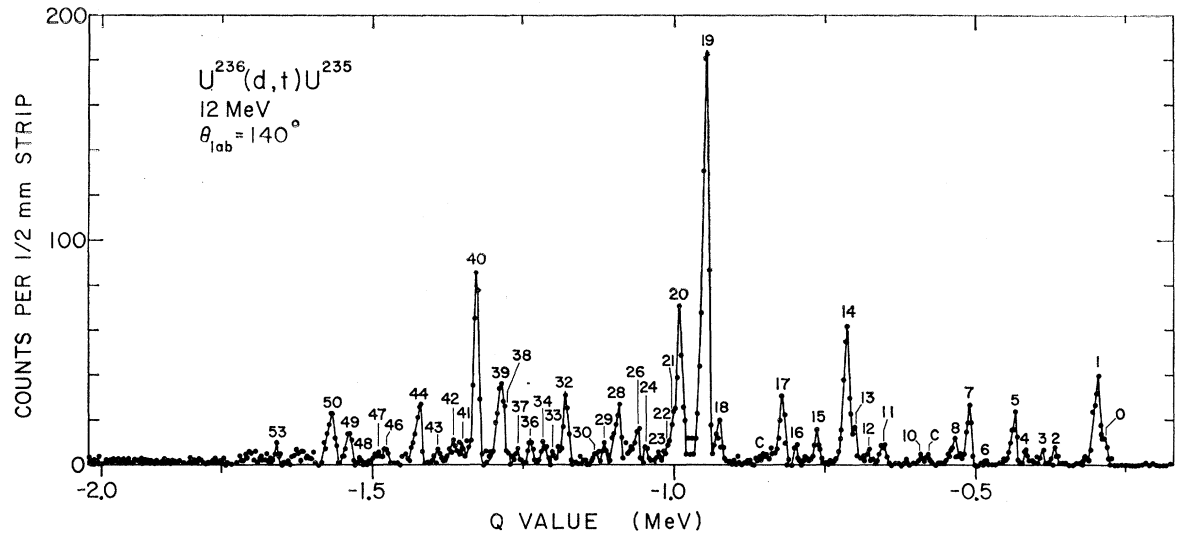

FIG. 3. Spectrum of tritons observed at 140° from a U^{236} target bombarded with a 12-MeV deuteron beam. Contaminant peaks are labeled C.

The value 0.70 was used for the ratio of actual to Coulomb scattering at 90° to the beam. This ratio was calculated with the optical-model potentials used by Macefield and Middleton[20] for deuteron scattering on uranium at 12 MeV and agrees well with the ratio[27] 0.70±0.03 measured under these conditions. In order to determine the bombarding energy (which is needed for absolute measurements of Q), a short exposure was also taken during each experiment to measure the energy of the elastically scattered deuterons.

The exposures for the (d, p) and (d, t) reactions required between 5000 and 10 000 μC of charge. Beam currents up to 0.5 μA were used. Because of the low cross sections, some of the exposures required 12 h or more. Several different U^{234} targets were used but only one U^{236} target. Exposures were made at observation angles of 90° to 140° and at 12-MeV bombarding energy.

For the Coulomb-excitation measurements, inelastic scattering data were recorded at 9-MeV bombarding energy at several angles between 120° and 140°. For some of the data, short exposures and long exposures were made to record the elastic and inelastic groups in such a way that the plates could be counted with the same scanning area. In the other portions of the data only one exposure was taken. The ratio of the elastic yields was then obtained by counting the data with different areas of scan. Careful attention was paid to the size of the scanned areas.

IV. EXPERIMENTAL RESULTS

Figures 2 and 3 show the results of (d, p) and (d, t) exposures obtained at 140°. The abscissa has been converted to Q value. Table II lists the excitation energies and differential cross sections obtained at 90° and 140° for the levels observed in the (d, p) and (d, t) reactions.

The ground-state Q values were measured to be 3.075±0.007 MeV for the $U^{234}(d, p)U^{235}$ reaction and −0.281±0.006 MeV for the $U^{236}(d, t)U^{235}$ reaction.[9]

V. DISCUSSION

A. Catalog of Experimental and Theoretical Signatures

As was noted in Sec. II, the differential cross sections for the population of the members of a rotational band based on a given single-particle state depend strongly upon the wave function of that state. Thus, the relative cross sections associated with each single-particle state give a characteristic signature and these are of great value in identifying the single-particle state. (The signatures are also affected by band mixing in some cases and this must be taken into account.) In the series of actinide elements which we have studied, we have experimentally identified many signatures of neutron single-particle states either when they have occurred at or near the ground state of an odd-A nucleus or when they have been positively identified through α- or β-decay studies.

Figure 4 shows the signatures measured experimentally (upper graph for each state) for 12 neutron single-particle states which we have observed and also shows the theoretical signatures calculated from both Nilsson-type (graphs labeled N) and Rost-type (labeled W-S) wave functions and the DWBA theory of single-particle transfer. The DWBA calculations were discussed above in Sec. II. In each case, the differential cross section summed over all the members of each rotational band is normalized to 1.0. The

[27] N. Williams (private communication).

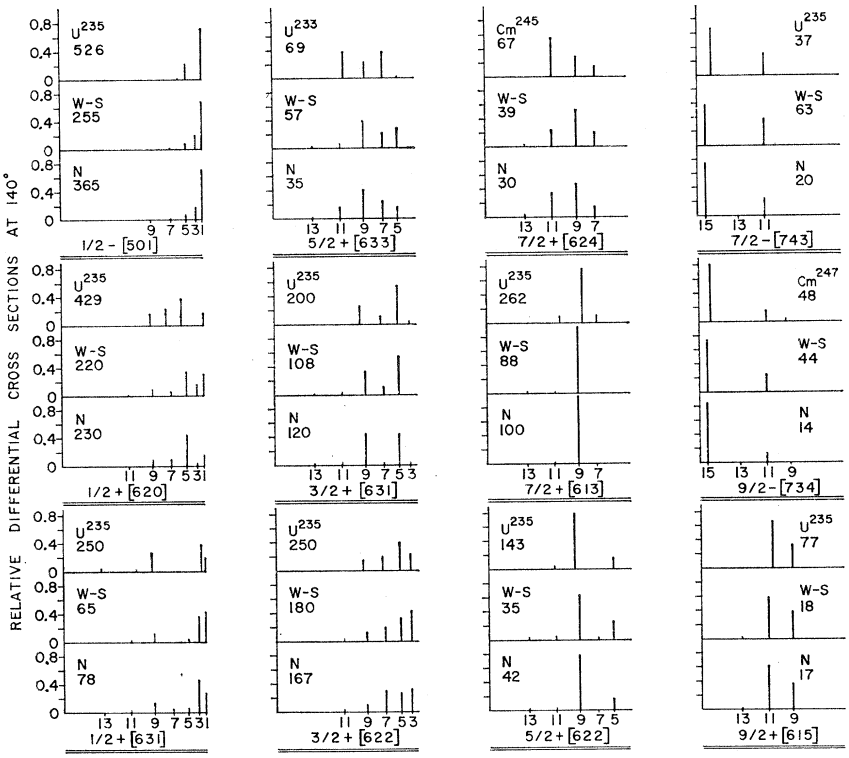

FIG. 4. A catalog of signatures (i.e., sets of expected relative differential cross sections) for most of the single-particle states studied in the present work. The experimentally determined signatures were measured at 140° and 12-MeV bombarding energy. The theoretical signatures were calculated with Nilsson (designated N) and Rost-type (designated W-S) deformed wave functions. The DWBA parameters are given in Table I. For convenience in plotting the bar graphs, the total cross section measured or calculated for each band has been normalized to unity; the actual value of the total cross section (in μb/sr) is shown by the number on each graph.

number stated in each of the bar graphs is the sum of the differential cross sections (in μb/sr) for all rotational levels in the band.

It can be seen in Fig. 4 that while both the Rost and Nilsson calculations describe the major features of the signatures (i.e., if a rotational level is predicted to have a large cross section, it usually does), both calculations fail frequently in describing the finer details. For states at low excitation energy, especially for the weak ones, the spectroscopic factors sometimes disagreed by a factor of 2 in either direction. This is undoubtedly partly due to uncertainty in the optical-model parameters and uncertainties in the single-particle wave functions. Also, it is known that large effects can be produced by inelastic scattering mechanisms, as was pointed out by Iano and Austern[28] and by Kunz, Rost, and Johnson.[29] We did not include inelastic scattering effects in our calculations. In the (d, p) reactions, we note a tendency for the measured absolute cross section to be about twice the calculated cross sections. This may be related to the situation reported by Siemssen and Erskine[30,31] in the $W^{182}(d, p)W^{183}$ reaction, where the measured differential cross sections were found to be about twice as large as the cross sections calculated when optical-model parameters were used that fit the elastic scattering data. In spite of difficulties with the absolute cross sections, we found for U^{235}, as others[32–34] have usually found in deformed heavy nuclei, that the observed relative differential cross sections within one rotational band agree moderately well with the theory.

B. Assignment of Single-Particle Levels in U^{235}

The procedure we have used to assign the observed levels in U^{235} in terms of the Nilsson single-particle model is as follows.

We first attempt to identify a state by means of its signature. Besides the theoretical signatures obtained from the Nilsson and Rost calculations, we also make use of the library of experimentally determined signatures shown in Fig. 4. We also make the fullest possible use of the information published on levels in U^{235}. Besides examining cross-section ratios to presumed members of a rotational band, we also demand that the members of the band be reasonably spaced in energy (i.e., we demand a reasonable value of $\hbar^2/2\vartheta$).

At this point in the analysis, we make qualitative use of the ratio R_κ of Eq. (4), to decide whether each state is a particle or hole state. This gives us a single-particle scheme. Next we calculate the pairing effects and obtain an extracted single-particle spectrum. We used this

[28] P. J. Iano and N. Austern, Phys. Rev. **151**, 853 (1966).
[29] P. D. Kunz, E. Rost, and R. R. Johnson, Phys. Rev. **177**, 1737 (1969).
[30] R. H. Siemssen and J. R. Erskine, Phys. Rev. Letters **19**, 90 (1967).
[31] R. H. Siemssen and J. R. Erskine, Phys. Rev. **146**, 911 (1966).
[32] J. R. Erskine, Phys. Rev. **138**, B66 (1965).
[33] M. N. Vergnes and R. K. Sheline, Phys. Rev. **132**, 1736 (1963).
[34] D. G. Burke, B. Zeidman, B. Elbek, B. Herskind, and M. Olesen, Kgl. Danske Videnskab. Selskab, Mat.-Fys. Medd. **35**, No. 2 (1966).

TABLE II. Energy levels in U^{235} and their excitation energies, differential cross sections in (d, p) and (d, t) reactions, orbital assignments, spin assignments, and confidence levels.

Level No.	Excitation (keV)	$d\sigma(d,p)/d\Omega$ (μb/sr) 90°	$d\sigma(d,p)/d\Omega$ (μb/sr) 140°	$d\sigma(d,t)/d\Omega$ (μb/sr) 90°	$d\sigma(d,t)/d\Omega$ (μb/sr) 140°	Assignment Orbital	Assignment I	Confidence level
0	0.0	88±20	48±11	39±18	27±4	$\frac{1}{2}$+[631]	1/2	*A*
1	13.2±0.5	179±30	91±15	114±30	81±6	$\frac{1}{2}$+[631]	3/2	*A*
2	80±2	20±3	20±7	12±6	12±3	$\frac{1}{2}$+[631]	7/2	*A*
3	102±2	14±2	8±4	20±8	12±4	$\frac{7}{2}$−[734]	11/2	*A*
4	128±1	22±3	22±6	11±8	13±4	$\frac{5}{2}$+[622]	5/2	*A*
5	149±1	81±5	65±9	28±15	47±9	$\frac{1}{2}$+[631]	9/2	*A*
6	(194±5)	<4	<5	<5	4±2	$\frac{1}{2}$+[631]	11/2	*A*
7	225.5±1	125±8	109±13	31±14	52±6	$\frac{5}{2}$+[622]	9/2	*A*
8	252±2	7±2	25±7	7±4	25±4	$\frac{7}{2}$−[743]	15/2	*A*
9	293±3	<4	13±4	<3	8±2	$\frac{1}{2}$+[631]	13/2	*A*
10	(332±3)	<4	5±3	<3	4±2	$\frac{5}{2}$+[633]	5/2	*C*
11	367±3	8±2	13±4	17±4	17±3	$\frac{5}{2}$+[633]	7/2	*B*
12	392±2	<5	<5	21±5	11±2	$\frac{3}{2}$+[631]	3/2	*A*
13	415±2	64±19	46±5	34±7	31±5	$\frac{5}{2}$+[633]	9/2	*C*
14	427±2	57±17	21±3	99±11	114±9	$\frac{3}{2}$+[631]	5/2	*A*
15	474±3	8±4	10±3	13±4	25±4	$\frac{3}{2}$+[631]	7/2	*A*
16	509±3	44±6	45±5	9±3	11±3	$\frac{7}{2}$+[624]	9/2	*C*
17	533±3	15±4	9±3	48±6	54±10	$\frac{9}{2}$+[631]	9/2	*A*
18	638±3	(7±4)	<3	20±5	38±6	$\frac{5}{2}$−[752]	5/2	*C*
19	659±2	26±7	23±9	320±45	393±20	$\frac{1}{2}$−[501]	1/2	*B*
20	703±3	34±6	23±10	111±14	127±22	$\frac{1}{2}$−[501]	5/2, 3/2	*B*
21	716±5	4	(6±3)	(20±12)	(20±12)	$\frac{5}{2}$−[752]	9/2	*C*
22	(725±5)	<4	4±2	(10±5)	(10±5)	$\frac{1}{2}$−[501]	7/2	*C*
23	735±5	<4	14±7	17±6	(6±4)			
24	755±5	<10	(12±6)	15±7	9±4			
25	768±3	58±8	41±12	25±10	<7			
26	776±4	<7	<10	24±6	34±10	$\frac{5}{2}$−[752]	11/2	*C*
27	795±3	26±5	22±11	21±7	<7			
28	804±4	<5	27±12	18±7	58±14			
29	827±3	35±7	38±13	25±7	13±7			
30	845±2	73±10	51±16	<5	(7±3)			
31	866±3	26±6	17±10	5±2	<5			
32	893±3	92±11	66±15	40±11	55±6			
33	(914±5)	<7	<20	10±6	8±4			
34	927±4	<7	<12	11±6	16±3	$\frac{5}{2}$−[752]	15/2	*C*
35	916±4	22±6	22±10	9±3	16±3			
36	(968±5)	<7	<15	11±6	9±3			
37	995±3	21±9	17±10	45±14	52±9			
38	1001±4	18±8	26±13	20±9	45±8			
39	1039±2	75±14	36±14	118±21	167±15			
40	1061±5	27±8	10±4	22±10	14±5			
41	1075±5	<15	<8	20±8	18±5			
42	1098±6	<15	<8	17±6	10±3			
43	1133±2	40±15	24±12	44±12	56±6			
44	(1140±5)	30±15	15±10	<10	<10			
45	1191±2	135±20	34±15	23±15	13±4			
46	1202±2	67±15	62±24	<8	7±3			
47	1236±3	37±15	30±15	<8	<4	$\frac{7}{2}$+[613]	7/2	*C*
48	1246±3	<20	<15	19±10	26±5			
49	1255±2	122±48	78±9	<12	<8	$\frac{1}{2}$+[620]	1/2	*C*
50	1273±2	290±66	207±38	53±20	55±7	$\frac{7}{2}$+[613]	9/2	*B*
51	1318±3	217±29	167±30	<5	<8	$\frac{1}{2}$+[620]	5/2	*B*
52	(1340±7)	25±15	25±15	<5	<8	$\frac{7}{2}$+[613]	11/2	*C*
53	1361±3	118±11	109±25	13±5	25±8	$\frac{1}{2}$+[620]	7/2	*B*
54	1392±2	86±13	59±22	<5	<8	$\frac{3}{2}$+[622]	3/2	*B*
55	1405±4	111±12	76±27	<5	<8	$\frac{1}{2}$+[620]	9/2	*C*

TABLE II. (*Continued*).

Level No.	Excitation (keV)	$d\sigma(d,p)/d\Omega$ (μb/sr) 90°	140°	$d\sigma(d,t)/d\Omega$ (μb/sr) 90°	140°	Assignment Orbital	I	Confidence level
56	1423±4	126±12	101±25	<5	<8	$\frac{3}{2}$+[622]	5/2	*B*
57	(1438±7)	29±7	25±15	<5	<8	$\frac{9}{2}$+[615]	9/2	*C*
58	1471±4	47±8	50±22	<5	<8	$\frac{3}{2}$+[622]	7/2	*C*
59	1495±4	32±6	51±23	<5	<8	$\frac{9}{2}$+[615]	11/2	*C*
60	1525±4	46±6	38±20	<5	<8	$\frac{3}{2}$+[622]	9/2	*C*
61	1618±5	126±25	88±21	<5	<8			

extracted spectrum, together with occupation probabilities obtained from the pairing calculation, to make semiquantitative estimates of Coriolis interactions and expected modifications of the single-particle signatures.

We also assume that the same extracted single-particle level scheme obtained from the U^{235} holds for both U^{234} and U^{236}. With this assumption, we can compute the factors R_κ, and this gives an additional check on the plausibility of our assignments.

We shall use the labels *A*, *B*, and *C* to denote the degree of certainty involved in our assignments of both single-particle states and the individual members of the rotational bands based on those single-particle states.

The label A is used to denote well-established single-particle states. These are states that are well characterized in terms of their signatures. We consider a single-particle state to be well characterized in terms of its signature when that state has been identified by means of decay-scheme studies in at least one of the actinides, and we have experimentally found that its signature corresponds to the calculated one. This label is also applied to states for which the reaction data are not definitive but for which an assignment can be made on the basis of independent data (e.g., Coulomb excitation or decay scheme) and the reaction studies are consistent with that assignment. An additional and important requirement is that the signature have one extremely prominent peak or at least two moderately prominent ones.

We consider a level assignment to be of confidence level *A* when the peak corresponding to it is at least moderately prominent in the spectrum and both the R_κ and the cross-section ratio $\sigma(90°)/\sigma(140°)$ are consistent with our assignment. Additionally, the peaks expected for other members of its rotational band must be present in our experimental spectrum.

The label B is used to denote probable single-particle states. These are states that have not been independently observed in at least one actinide nucleus. We maintain the condition that the signature must correspond to the theoretically expected one. Individual level assignments are downgraded from *A* to *B* when the value of either R_κ or the cross-section ratio $\sigma(90°)/\sigma(140°)$ disagrees considerably with our assignment.

The label C is used to denote plausible single-particle states. These are states that do not have prominent peaks and are assigned solely on the basis of systematics (i.e., the excitation energy is predicted from either the Nilsson or Rost calculation or from the experimentally known energy in some other actinide nucleus). In the absence of compelling independent information, this label is also used for *individual levels* populated with low cross section.

It should be made clear that our assignments are prejudiced to some extent by model considerations (e.g., the $\frac{1}{2}$−[501] assignment). It should also be noted that the lines of demarcation between the categories *A*, *B*, and *C* are not always sharp, and subjective judgements are involved in the meaning of phrases such as "correspond to," "consistent with," "moderately prominent," etc.

In the discussion of individual levels, we employ a notation which we have found to be convenient. The parenthetic number usually following a stated level energy is the label attached to that level in Table II and Figs. 2 and 3.

Unless otherwise stated, all references to (*d*, *p*) and (*d*, *t*) studies on other actinide nuclei are to our investigations, a report of which is being prepared. As mentioned above, preliminary reports have already been made.[6,9,10] References to the literature are made to the compilations of Hyde, Perlman, and Seaborg[35] and of Lederer, Hollander, and Perlman[36] unless otherwise stated. The level assignments made in the present study are given in Fig. 5, an energy level diagram of U^{235}. A detailed discussion of these assignments follows.

1. $\frac{1}{2}$+[631]; *A*

In the α decay[1–3] of Pu^{239}, all the levels of this band are populated by the favored transition and are well identified. On this basis we have assigned the levels at 0(0), 13.2(1), 80(2), 149(5), 194(6), and 293(9) keV as $I=\frac{1}{2}, \frac{3}{2}, \frac{7}{2}, \frac{9}{2}, \frac{11}{2}$, and $\frac{13}{2}$ levels, respectively, of

[35] E. K. Hyde, I. Perlman, and G. T. Seaborg, *The Nuclear Properties of the Heavy Elements. II. Detailed Radiactive Properties* (Prentice-Hall, Inc., Englewood Cliffs, N.J., 1964).

[36] C. M. Lederer, J. M. Hollander, and I. Perlman, *Table of Isotopes* (John Wiley & Sons, Inc., New York, 1967).

this rotational band. The signature agrees well with the theoretical one. We have observed[6,8] this state as the ground state in U^{237} with the $U^{236}(d, p)U^{237}$ and $U^{238}(d, t)U^{237}$ reaction. The l values and the cross-section ratios $\sigma(d, p)/\sigma(d, t)$ are in good agreement with this assignment for all except the $I=\frac{11}{2}$ level, for which the cross section is quite low. Except for this, we feel that the assignments of all levels of this rotational band are well established and label them as classification A.

2. $\frac{7}{2}-[743]$; A

This state is not well populated in (d, p) and (d, t) reactions. The only observable transitions go to the $I=\frac{11}{2}$ and $\frac{15}{2}$ levels. Newton,[4] using Coulomb excitation of U^{235}, has identified the $I=\frac{7}{2}$, $\frac{9}{2}$, and $\frac{11}{2}$ levels at 0, 49, and 103 keV. A more recent Coulomb-excitation study of these levels up to $I=25/2$ has been made by Stephens *et al.*[5] In the α decay[2] of Pu^{239}, transitions to these levels have been seen as well as to the $I=\frac{13}{2}$ and $\frac{15}{2}$ levels at 170 and 248 keV. We assign the level seen at 102 keV to the $I=\frac{11}{2}$ state and the level seen at 252 keV to the $I=\frac{15}{2}$ state since the energies correspond to those observed in the α-decay studies. Although the cross sections are small, they are consistent with the calculated signature for this state.

3. $\frac{5}{2}+[622]$; A

This band was observed in the α decay of Cm^{245} and was identified[37] as one built on the ground state of Pu^{241}. We have determined its signature with the reaction $Pu^{240}(d, p)Pu^{241}$ and $Pu^{242}(d, t)Pu^{241}$. The levels we observe at 128(4) and 225.5(7) keV in U^{235} are assigned as the $I=\frac{5}{2}$ and $\frac{9}{2}$ members of the $\frac{5}{2}+[622]$ rotational band. Their observed signature and the values of the ratio $\sigma(90°)/\sigma(140°)$ are in excellent agreement with those expected for this assignment. Baranov *et al.*[1] observed both these levels in the α decay of Pu^{239}. However, they assumed that the 129-keV level was the band head of the $\frac{5}{2}+[633]$ state and left the 224-keV level unassigned. On the basis of α-decay studies alone, it is not possible to distinguish between the $\frac{5}{2}+[622]$ and $\frac{5}{2}+[633]$ single-particle states. Our reaction studies show conclusively that this band has the signature of the single-particle state $\frac{5}{2}+[622]$ and not the signature of the $\frac{5}{2}+[633]$ state, which is quite different as seen in Fig. 4. This assignment agrees with the results of α-γ and γ-γ coincidence studies of the decay of Pu^{239} made by Ahmad[2] and by Cline.[3]

From the known energies of the $\frac{5}{2}$, $\frac{7}{2}$, and $\frac{9}{2}$ members of this band, we compute that the $\frac{11}{2}$ member of this band should be at 291 keV. Therefore, the peak seen at 293(9) keV and assigned as the $\frac{13}{2}$ member of the $\frac{1}{2}+[631]$ band may well be partly due to the $\frac{11}{2}$ member of this band. We label the $\frac{5}{2}$ and $\frac{9}{2}$ assignments as A.

[37] A. M. Friedman and J. Milsted, Phys. Letters **21**, 179 (1966).

4. $\frac{5}{2}+[633]$; B

Since this state has small cross sections for the transitions to all rotational levels, it is very difficult to identify it on the basis of (d, p) and (d, t) data alone. We have observed the signature of the $\frac{5}{2}+[633]$ state in (d, t) reactions to the ground states of U^{233} and Th^{231} and expect on the basis of systematics that this state should be a hole state within 400 keV of the ground state of U^{235}. In a study of the α decay of Pu^{239}, Ahmad[2] has found a $K=\frac{5}{2}$ band in U^{235} and assigned it to the $\frac{5}{2}+[633]$ single-particle state. He found $I=\frac{5}{2}$, $\frac{7}{2}$, and $\frac{9}{2}$ levels at 332.9, 367.3, and 414.7 keV. The levels we observed at 332(10), 367(11), and 415(13) keV are consistent with this assignment as the $I=\frac{5}{2}$, $\frac{7}{2}$, and $\frac{9}{2}$ rotational levels of this state. Within the large errors in the measured cross sections of these levels, they fit the expected signatures, the angular dependence, and the ratio $\sigma(d, p)/\sigma(d, t)$. Rickey and Britt[38] have also observed this state with the $U^{233}(t, p)U^{235}$ reaction. The (t, p) reaction strongly populates the $\frac{5}{2}+[633]$ band since this is the ground state of the target.

5. $\frac{3}{2}+[631]$; A

This single-particle state has been identified in U^{233} by β-decay studies of Pa^{233}. We have experimentally determined its signature with the reaction $U^{234}(d, t)U^{233}$. The levels at energies 392(12), 427(14), 474(15), and 533(17) keV are assigned as the $I=\frac{3}{2}$, $\frac{5}{2}$, $\frac{7}{2}$, and $\frac{9}{2}$ members of this rotational band. These levels have also been assigned by Ahmad[2] as the $\frac{3}{2}+[631]$ rotational band in α decay and in α-γ coincidence studies. The cross sections for these levels conform quite well to the expected signature of the $\frac{3}{2}+[631]$ band. Furthermore, the ratios $\sigma(90°)/\sigma(140°)$ and $\sigma(d, p)/\sigma(d, t)$ are consistent with this assignment. We feel that all of the levels are well established and place them in category A.

6. $\frac{7}{2}+[624]$; C

The $\frac{7}{2}+[624]$ state should appear in U^{235} roughly 200 keV above the $\frac{5}{2}+[622]$ state, since this is the observed[6,39] spacing between these two states in U^{239}, Pu^{241}, and Cm^{243}. The small cross sections and the strong Coriolis mixing of the levels have made the $\frac{7}{2}+[624]$ band in U^{235} very difficult to identify on the basis of evidence from (d, p) and (d, t) reactions alone. The $\frac{5}{2}+[633]$ band head is nearly at the same energy as the expected band head of the $\frac{7}{2}+[624]$ state and the allowed nature of the Coriolis mixing between these levels guarantees strong mixing. We originally suggested[6] that the $\frac{7}{2}+[624]$ band head was composed of the levels at 415 and 475 keV. However, Ahmad showed[2] that these levels belonged to the $\frac{5}{2}+[633]$ and $\frac{3}{2}+[631]$ bands. We now believe that the 509-keV

[38] F. A. Rickey and H. C. Britt, Bull. Am. Phys. Soc. **12**, 522 (1967).

[39] R. K. Sheline, W. N. Shelton, T. Udagawa, E. T. Jurney, and H. T. Motz, Phys. Rev. **151**, 1011 (1966).

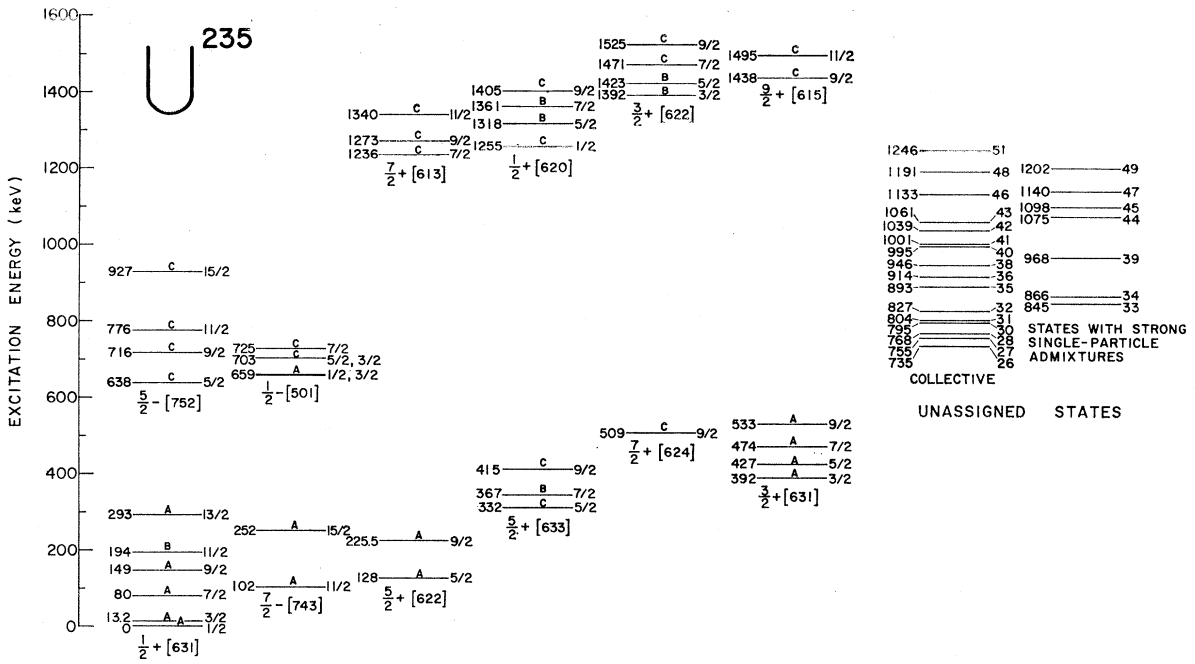

FIG. 5. Energy level diagram of U^{235}. Wherever possible the levels have been assigned to rotational bands whose asymptotic quantum numbers are given below each band. The measured excitation energies (in keV) and assigned spins are given. The confidence level of each assignment is denoted by the letters *A* (well established), *B* (probable), and *C* (plausible). The unassigned states that appear to have strong single-particle admixtures are shown separately from the other unassigned states, most of which are probably vibrational states.

level, seen most strongly in the (d, p) spectrum, is the $I=\frac{9}{2}$ level of the $\frac{7}{2}+[624]$ band. Our confidence level is only *C* for this assignment.

7. $\frac{5}{2}-[752]$; *A*

This state has been observed by Stephens *et al.*[5] in Coulomb excitation of U^{235}. Their data establish a rotational band with spins to $\frac{13}{2}$ and with levels at 633, 671, 720, 778, and 851 keV. They have assigned this band to the $\frac{5}{2}-[752]$ configuration, which is expected to be a hole state in U^{235}. On the basis of our reaction data alone, it would not be possible to assign this state. Our levels, Nos. 18, 21, and 26 at 638±3, 716±5, and 776±4 keV, respectively, appear to be hole states and may be the levels observed by Stephens *et al.* We give confidence *C* for the levels which we have observed. From the energies of these states one predicts that the $\frac{15}{2}$ state of this band is at 932 keV. Level 34 at 927±4 keV appears to be a hole state and is consistent with the assignment to the $I=\frac{15}{2}(C)$ level of this band. The theoretical signature shows that in this band the member with the largest cross section corresponds to the $I=\frac{15}{2}$ level, which is consistent with our assignment.

8. $\frac{1}{2}-[501]$; *A*

The $\frac{1}{2}-[501]$ state has been seen as a hole state in many of the actinide nuclei we have studied,[6] although we have never observed it as a ground state. The theoretical signature indicates a large cross section in the (d, t) reaction to the $I=\frac{1}{2}$ level. The level at 659(19) keV, which has a very large cross section in the (d, t) reaction, and also the one at 703(20) keV are assigned to this state. The DWBA calculations indicate that the cross-section ratio for an $l=1$ transition populating a $J\pi=\frac{1}{2}-$ level should be $\sigma(90°)/\sigma(140°)=0.94$ and our measurements indicate that the value is 0.8±0.1 for the 659-keV level. Bjørnholm *et al.*[40] report a level in U^{235} at 650±20 keV to which they assign a spin and parity $J\pi=\frac{1}{2}-$. The strong state we see at 659 keV, which appears to be the spin-$\frac{1}{2}$ state of the $\frac{1}{2}-[501]$ band, may be the state reported by these authors. It is difficult to make spin assignments for levels in this band other than the one at 659 keV. We believe it is most likely that the 703-keV level is a doublet consisting of the $I=\frac{3}{2}$ and $\frac{5}{2}$ states. A rotational constant of about 7 keV and a decoupling constant $a=0.8$ accounts for this spacing. This value for the decoupling constant is consistent with the values 0.7–0.8 calculated from Nilsson or Rost wave functions. Another possibility, which we feel is less likely, is that both the 659- and 703-keV levels may be doublets formed from the $I=\frac{1}{2}$, $\frac{3}{2}$ and $I=\frac{5}{2}$, $\frac{7}{2}$ states. The decoupling constant in this situation would be close to $a=-1$. A negative decoupling constant could result from mixing of the $\frac{1}{2}-[501]$ state with the $\frac{1}{2}-[770]$

[40] S. Bjørnholm, M. Lederer, F. Asaro, and I. Perlman, Phys. Rev. **130**, 2000 (1963).

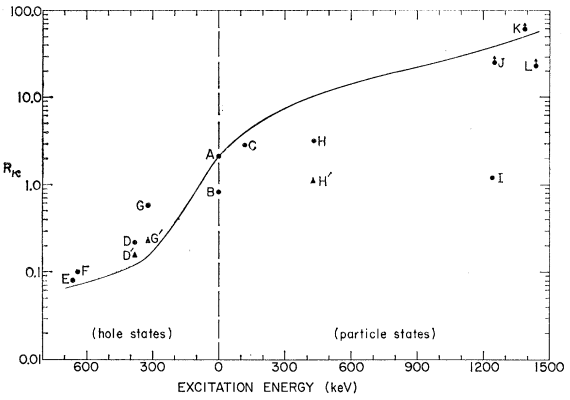

FIG. 6. The ratio R_κ of (d, p) to (d, t) spectroscopic factors for the rotational bands observed in U^{235}. The experimental values indicated by the circular points were obtained whenever possible by combining the cross-section ratios $\sigma(d, p)/\sigma(d, t)$ for several members in the rotational band. Effects of reaction mechanism were removed through the use of the DWBA calculations described in the test. The theoretical values of R_κ indicated by the solid line were obtained with pairing theory. For those states for which it was considered important, the theoretical calculations have been approximately corrected for Coriolis effects. These corrected theoretical ratios are indicated by the triangular points and primed labels as explained in the text. The letters refer to the following single-particle states: $A=\frac{1}{2}+[631]$, $B=\frac{7}{2}-[743]$, $C=\frac{5}{2}+[622]$, $D=\frac{3}{2}+[631]$, $E=\frac{1}{2}-[501]$, $F=\frac{5}{2}-[752]$, $G=\frac{5}{2}+[633]$, $H=\frac{7}{2}+[624]$, $I=\frac{7}{2}+[613]$, $J=\frac{1}{2}+[620]$, $K=\frac{3}{2}+[622]$, and $L=\frac{9}{2}+[615]$.

state. The latter state (not yet located) is expected to lie near the $\frac{1}{2}-[501]$ state and $\Delta N=2$ mixing would then lower the decoupling constant. The 652- and 658-keV states, with spins $\frac{1}{2}-$ or $\frac{3}{2}-$, reported by Lederer[41] would tend to support this latter interpretation. Our (d, t) data did not show the 652-keV level, but certainly would have shown it if it came from the $\frac{1}{2}-[501]$ state. Therefore, we prefer the first interpretation. However, further measurements are needed to confirm this.

9. $\frac{7}{2}+[613]$; C

The calculated signature of this state shows a large cross section for the transition to the $I=\frac{9}{2}$ level, a smaller one to the $\frac{11}{2}$ level, and almost no cross section for the transition to the $\frac{7}{2}$ level. Both the Nilsson and Rost calculations of energy versus deformation indicate that the energy of this state should increase relative to that of the $\frac{1}{2}+[620]$ state as the nuclear deformation is increased. The $I=\frac{9}{2}$ level of the $\frac{7}{2}+[613]$ state has been seen in many of the isotopes we have studied.[6] It is 75 keV above the $I=\frac{1}{2}$ level of the $\frac{1}{2}+[620]$ state in the curium isotopes. It has also been seen 166 keV above the $I=\frac{1}{2}$ level in Cf^{249}, which was studied[42] in the α decay of Fm^{253}. For this reason the levels at 1236(47), 1273(50), and 1340(52) keV are assigned to the $I=\frac{7}{2}(C)$, $\frac{9}{2}(C)$, and $\frac{11}{2}(C)$ rotational levels of the $\frac{7}{2}+[613]$ state. There may be another level very close to the 1273-keV level excited by the (d, t) reaction, since if our assignment is correct the (d, t) cross section is too large. The angular dependence of the cross sections is consistent with these assignments, and the R_κ ratio indicates that all are particle states.

10. $\frac{1}{2}+[620]$; B

This state has been identified[43] in Cm^{247} as the one on which the rotational band populated by the unhindered α decay of Cf^{251} is built. We have observed its signature in Cm^{245}, Cm^{247}, and Cm^{249} (in the latter of which it is the ground state) with the (d, p) reaction. In U^{235}, of course, the signature at this high excitation energy may differ somewhat from cases in which it is nearer the ground state. The spin-$\frac{1}{2}$ rotational level is probably too close to the $\frac{9}{2}$ level of the $\frac{7}{2}+[613]$ state to be clearly resolved. However, the spins $I=\frac{5}{2}(B)$, $\frac{7}{2}(B)$, and $\frac{9}{2}(C)$ were assigned to the levels 1318(51), 1361(53) and 1405(56) keV, respectively, and the energies of the $K=\frac{1}{2}$ rotational band were fitted with a rotational constant of 5.52 keV and a decoupling constant $a=+0.11$. The cross section of the transition to the $I=\frac{3}{2}$ level is calculated to be very small, and it is not surprising that we do not observe it. The value of the rotational constant and decoupling constant found[36] in the α-decay studies of Fm^{255} were $\hbar/2\vartheta=6.4$ keV and $a=+0.29$, respectively, for this band. However, in U^{235} at a higher excitation energy these parameters could be changed somewhat by mixing with other configurations. We are more certain of the existence of the $\frac{1}{2}+[620]$ state than we are of the detailed level assignments to the band.

11. $\frac{3}{2}+[622]$; B

The energy of this state is close to the energy of the $\frac{1}{2}+[620]$ state in the calculated single-particle level scheme. The levels at 1392(54), 1423(56), 1471(58), and 1525(60) keV have been assigned to the $I=\frac{3}{2}(B)$, $\frac{5}{2}(B)$, $\frac{7}{2}(C)$, and $\frac{9}{2}(C)$ rotational levels of this band. These energies fit, within the experimental errors, the spacings of a $K=\frac{3}{2}$ rotational band with a rotational constant of 6.36 keV, and the cross sections, in general, resemble the calculated signatures. To obtain detailed agreement one would, of course, have to consider mixing effects. For these levels, the angular dependences in the (d, p) and (d, t) reactions are consistent with our assignments, and the state has a very high value of the cross-section ratio $\sigma(d, p)/\sigma(d, t)$ as expected.

12. $\frac{9}{2}+[615]$; C

The calculated signature for this state consists of strong transitions to the $I=\frac{9}{2}$ and $\frac{11}{2}$ levels, the cross section for the spin-$\frac{11}{2}$ state being the larger. This rotational band has tentatively been identified[36] in Cf^{251} (in studies of the α decay of Fm^{255}) at about 400 keV above the $\frac{1}{2}+[620]$ state. Since the binding energy

[41] C. M. Lederer, in Ref. **36**, p. 432.

[42] I Ahmad, A. M. Friedman, R. F. Barnes, R. K. Sjoblom, J. Milsted, and P. R. Fields, Phys. Rev. **164**, 1537 (1967).

[43] A. Chetham-Strode and R. Silva, Nucl. Phys. **A107**, 645 (1968).

of the $\frac{9}{2}+[615]$ state decreases toward that of the $\frac{1}{2}+[620]$ state as the deformation increases, the $\frac{9}{2}+[615]$ state is expected to lie only a few hundred keV above the $\frac{1}{2}+[620]$ state in U^{235}. The levels at 1438(57) and 1495(59) keV have cross sections and angular dependences that fit the expected signatures of the $I=\frac{9}{2}(C)$ and $\frac{11}{2}(C)$ rotational levels of this band within our experimental errors. They also appear to be particle states. On this basis they are assigned to the $\frac{9}{2}+[615]$ state. However, without any other evidence, we must regard the assignment as only plausible.

C. Comparison of Theoretical and Experimental Values of R_κ

There is fair agreement, as can be seen in Fig. 6, between the calculated and experimental values of R_κ, the ratio of (d, p) to (d, t) spectroscopic factors. This ratio has been used as a tool in making our assignments of observed levels. We note that this ratio indicates that the single-particle state $\frac{7}{2}-[743]$ (point B in Fig. 6) is somewhat less occupied than is the state $\frac{1}{2}+[631]$ (point A). This may be explained by arguing that the $\frac{7}{2}-[743]$ state occurs at a somewhat lower energy in U^{236} than does the state $\frac{1}{2}+[631]$. The justification for this argument is that in U^{237} the $\frac{7}{2}-[743]$ state has been observed[44] at an excitation of 274 keV and the $\frac{1}{2}+[631]$ is the ground state in that nucleus.

Calculated values of R_κ are modified by Coriolis effects which can be fairly large for the single-particle states $\frac{3}{2}+[631]$ and $\frac{5}{2}+[633]$ and extremely large for the single-particle states $\frac{7}{2}+[624]$. Coriolis-interaction matrix elements that provide a good fit to the experimentally determined energies were obtained. When these are used to correct the theoretical ratio R_κ for the above levels, this theoretical ratio changes to the values indicated by the triangular points denoted as D', G', and H' in Fig. 6. We feel that these calculated values are more nearly correct, but we have not made an exhaustive study of the Coriolis effects.

For state I, which has been assigned as the $\frac{9}{2}$ member of the $\frac{7}{2}+[613]$ rotational band, the value of R_κ is 30 times the calculated value. This discrepancy may possibly be explained by postulating an unresolved level which shows up strongly in the (d, t) reaction. Another possibility is that the wave function of the 1273-keV level may not be pure and may contain some hole-state admixtures.

We have used wave functions obtained with the method described by Chasman[45] to compute the factors R_κ. This procedure was followed in order to calculate the spectroscopic factors for the populations of possible states that are pairing excitations[45] built on the various single-particle states. We have found that the calculated spectroscopic factors of transitions to such states are no more than ~1% of the spectroscopic factors of those to the single-particle states. Therefore, we cannot describe any of the unassigned levels we have observed as pairing vibrational levels (seniority-zero excited states).

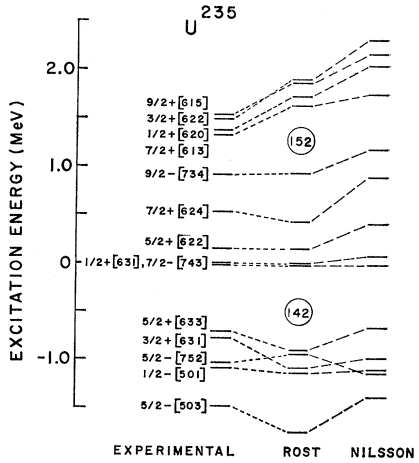

FIG. 7. Comparison of single-particle energies. The experimental energies have been corrected for pairing effects. The calculated values were obtained with Rost's coupled-channel code and Nilsson's new potential which includes a $P_4(\cos\Theta)$ term. It should be noted that in the Rost calculation the well-depth parameter V_0 is 500 keV greater for negative-parity states than for positive-parity states.

D. Unassigned States

Between 700- and 1500-keV excitation we observe 23 states that we have not assigned. Many of these have comparable (d, p) and (d, t) cross sections and therefore R_κ of Eq. (4) has a value of the order of unity. Since the ratio R_κ becomes either very large or very small for single-particle states at these excitation energies, we feel that states with $R\approx 1$ may be collective states. In U^{234}, and $I=1-$ state has been found[36] at 786 keV, a 0+ state at 810 keV, and 2+ states at 852 and 922 keV. A 2− state has been found[36] in U^{236} at 688 keV. It seems quite reasonable that many of the levels we have not assigned are vibrational excitations built on the single-particle states.

Lederer[41] and Bjørnholm *et al.*[40] have identified a level in U^{235} at 771 keV as having $I=\frac{1}{2}+$. Our level No. 25 at 768±3 keV has an angular dependence consistent with a $\frac{1}{2}+$ assignment. It is probably the level observed by Lederer and may be the β-vibrational state built on the $\frac{1}{2}+[631]$ single-particle state. The cross-section ratios $\sigma(d, p)/\sigma(d, t)$ at 90° for the $I=\frac{1}{2}$ level of the $\frac{1}{2}+[631]$ band (level No. 0) and level No. 25 at 768 keV are 2.3±0.4 and 2.3±0.8, respectively. This suggests that the wave function of the 768-keV state may be strongly admixed with that of level No. 0. Another interesting fact is that the cross section for populating level No. 25 is about one-half the cross section for populating level No. 0. This surprisingly

[44] I. Ahmad, A. M. Friedman, and J. P. Unik, Nucl. Phys. **A119**, 27 (1968).
[45] R. R. Chasman, Phys. Rev. **138**, B326 (1965).

large cross section also suggests large single-particle components in the wave function. It is tempting to try to do more with this 768-keV state. However, we note the following difficulty in confirming its assignment as a 0+ β-vibrational state built on the $\frac{1}{2}+[631]$ single-particle state. One might expect both the signature and the energy spacing of other levels within this β-vibrational band to be similar to those in the $\frac{1}{2}+[631]$ band near the ground state. However, a careful examination of our data failed to detect any obvious similarity between levels seen near the ground state and levels seen near the 768-keV state.

We have been able to rule out the possibility that the more prominent of these unassigned states are pairing excitations of the single-particle states. As mentioned earlier, such a description of the unassigned states leads to considerably smaller calculated spectroscopic factors than are observed for the prominent unassigned levels.

The observed ratios $\sigma(d, p)/\sigma(d, t)$ indicate that seven of the levels we have not assigned may have considerable admixtures of single-particle states in their wave functions. Level Nos. 30, 31, 44, and 46 may have strong particle-state admixtures, whereas level Nos. 36, 41, and 42 may have hole-state admixtures. Complex states of this type have been discussed by Soloviev and Vogel.[46] One expects many β- and γ-vibrational states built on the low-lying excited state to appear in this region of excitation. Stephens *et al.*[5] report evidence of collective vibrational states built on the $\frac{7}{2}+[743]$ single-particle state in the region of excitation in which we observe these unassigned states. Unfortunately, our experimental energy resolution was not sufficient to enable us to carry out detailed analysis of the properties of these unassigned states.

Further evidence of the complexity of the level structure of U^{235} above 700-keV excitation is found in the very recent work of Jurney.[47] He studied the $U^{234}(n, \gamma)U^{235}$ reaction with thermal neutrons and found a host of $J=\frac{1}{2}$ and $\frac{3}{2}$ states from 600- to 1500-keV excitation, many of which are not observed in our (d, p) and (d, t) study.

E. Extracted Single-Particle Level Scheme

In the process of analyzing our data, we obtained the extracted single-particle level scheme, i.e., one from which pairing effects have been removed. In Fig. 7, we compare the extracted level scheme with that obtained from the single-particle calculations of Nilsson and Rost. It can be seen that these single-particle models are fairly successful in reproducing the level orderings and energy spacing we have obtained from our analysis. It should be noted that the predictions of the Nilsson model can be brought into better agreement with the experimental data if the energy separations are uniformly scaled down by 25%; i.e., $\hbar\omega_0=31/A^{1/3}$ instead of the usual $\hbar\omega_0=41/A^{1/3}$.

[46] V. G. Soloviev and P. Vogel, Nucl. Phys. **A92**, 449 (1967).
[47] E. T. Jurney (to be published).

Several interesting features are evident in this experimentally determined neutron single-particle spectrum. (1) We see the single-particle states in the vicinity of the 152-neutron gap; levels are assigned on both sides of this gap. (2) We have found a large gap in the single-particle neutron spectrum at 142 neutrons. This gap is considerably larger in the extracted spectrum than it appears to be in the experimental energies. The reason for the increase in this gap is pairing. The pairing force has a small effect on the energies of particle states in U^{235}, but it causes a drastic lowering in the energies of hole states. From the extracted spectrum, we may surmise[48] that a low-lying 0+ excited state of the pairing-vibration type should be seen in U^{234} through the study of the $U^{236}(p, t)U^{234}$ reaction. (3) Another interesting feature of the single-particle spectrum is that there is a low density of single-particle states above 164 neutrons. This feature is more apparent in our reaction studies of the Cm and Pu isotopes than it is in the U^{235} data. In the present data, the existence of a gap at about 164 neutrons is suggested by Fig. 2 [the experimental (d, p) spectrum], where the number and strength of particle groups becomes small at the extreme left of the figure. Some but not all of this decrease in number of visible states could, of course, result from single-particle wave functions of the type for which most of the strength is in high-spin states which are not easily excited by the (d, p) reaction. This gap is much more apparent in our (d, p) data on heavier isotopes. A gap in the single-particle level scheme in the region near 164 neutrons could be seriously affecting the half-lives for spontaneous fission of the heaviest elements.

The extracted single-particle scheme obtained for U^{235} is a valuable test of single-particle potentials. The parameters of these potentials should be adjusted to bring them into agreement with our findings. The new Nilsson[49] calculation, which allows for hexadecapole as well as quadrupole deformations, is in quite good agreement with our findings when the parameters $\beta_2=0.23$, $\beta_4=-0.04$, $\kappa=0.065$, and $\mu=0.325$ are used. In addition to the single-particle states that have been identified, this calculation predicts that the $\frac{1}{2}-[761]$ and $\frac{11}{2}-[725]$ states should occur as particle states with roughly the same excitation energy as the $\frac{1}{2}+[620]$ state. It also predicts that the $\frac{13}{2}+[606]$ state should occur as a hole state in the vicinity of the $\frac{1}{2}-[501]$. While we have not assigned any of our observed levels to the $\frac{1}{2}-[761]$ state, we cannot exclude the possibility that some of the (d, p) strength near 1.3-MeV excitation is due to this state. Sheline *et al.*[39] report evidence for the $\frac{1}{2}-[761]$ state at 0.8-MeV excitation in U^{239}. However, in U^{235} we feel the available evidence is too weak to locate this state. The $\frac{11}{2}-[725]$ state has such a small calculated cross section that we do not expect to find it in our data. The $\frac{13}{2}+[606]$ state has a cal-

[48] J. Högaasen-Feldman, Nucl. Phys. **28**, 258 (1961).
[49] C. Gustafson, I. L. Lamm, B. Nilsson, and S. G. Nilsson, Arkiv Fysik **36**, 613 (1967).

culated (d, t) cross section which is about one-tenth that of the $\frac{1}{2}-[501]$ state. It may possibly appear in the data, although there is insufficient evidence to make an assignment.

VI. SUMMARY

We have obtained a considerable body of new information on the low-energy structure of U^{235}, in spite of some uncertainties involved in the analysis of the data from the (d, p) and (d, t) reactions. Together with other studies, the data obtained from the single-neutron-transfer reactions has led to an extensive knowledge of neutron single-particle states in U^{235}. The single-particle diagram obtained was presented in Fig. 7. The major result that emerges from our study is that the deformed-single-particle-potential models are semiquantitatively correct. We hope that our result will be used to adjust these models in such a way as to bring them into even better agreement with experiment. A well-known area of difficulty again pointed out by our studies is that of the absolute transfer cross section $\Theta_{Jl}{}^{DW}$. We have carried through our analysis mainly in terms of ratios of cross sections in order to bypass these difficulties.

In future papers of this series, we shall compare the information obtained from U^{235} with that obtained from other actinide nuclei.

ACKNOWLEDGMENTS

It is a pleasure to thank E. Rost and S. G. Nilsson for providing us with the most recent versions of their single-particle programs. We thank F. Stephens and I. Ahmad for valuable discussions. We also thank F. Rickey and H. Britt for sharing with us information they have obtained in experiments relevant to our present study. We are indebted to J. Lerner for preparing targets for our use and to M. Kastner for help in the difficult job of reducing the raw data.

APPENDIX: MEASUREMENT OF NUCLEAR DEFORMATIONS

Values of β were determined by Coulomb-excitation measurements with 9-MeV deuterons incident on a number of actinide nuclei. This energy is low enough so that the excitation of the 2+ state should be by pure Coulomb excitation. In practice, we made no attempt to measure the absolute cross sections, but instead measured the ratio of the cross section for excitation of the 2+ state to that for elastic scattering at the same angle. The latter cross section at this energy on such a high-Z nucleus can be assumed to be pure Rutherford scattering. The theoretical cross section, in mb/sr (lab), for exciting the 2+ state via Coulomb excitation depends on the deformation parameter β through the relation

$$d\sigma_{E2}=0.0565A_1[A_2/(A_1+A_2)]^2E_1A_2^{4/3}\beta^2 \times(1+0.16\beta)^2\,df(\theta,\Sigma). \quad (10)$$

In this expression, A_1 and A_2 are the mass numbers of the incident particle and the target, respectively, E_1 is the bombarding energy in MeV, and $df(\theta, \Sigma)$ is a tabulated function.[50] We derived expression (10) from the formulas given by Adler *et al.*[50] In doing so we have assumed that the nuclear radius is $R_0=1.2A^{1/3}$F, the value found to give the best fit in similar experiments on Th^{232} by Skurnik *et al.*[18] Our results are presented in Table III. A preliminary report on these measurements has previously been given.[7]

TABLE III. Nuclear deformations measured by means of Coulomb excitation.

Nucleus	β
U^{234}	0.25±0.01
U^{236}	0.265±0.02
Pu^{240}	0.276±0.002
Pu^{242}	0.284±0.01

It should be noted, however, that Eq. (10) in effect relates a macroscopic view of β to the nuclear quadrupole moment. This is only an approximation and one should really use the sum of the individual single-particle quadrupole moments weighted by the occupation probabilities V^2 for each state. However, we feel that the approximation is sufficiently accurate for our purposes.

[50] K. Alder, A. Bohr, T. Huus, B. Mottelson, and A. Winther, Rev. Mod. Phys. **28**, 432 (1956).